Nano Biomed Eng
2019, 11(2): 170-177. doi: 10.5101/nbe.v11i2.p170-177.

Research Article

Fabrication of ZnO:Al/Si Solar Cell and Enhancement its Efficiency Via Al-Doping

Khalid Haneen Abass, Musaab Khudhur Mohammed

Department of Physics, College of Education for Pure Sciences, University of Babylon, Iraq.

Corresponding authors. E-mail: Pure.khalid.haneen@uobabylon.edu.iq; pure.musaab.kh@uobabylon.edu.iq

Received: Dec. 31, 2018; **Accepted:** Apr. 30, 2019; **Published:** May 24, 2019.

Citation: Khalid Haneen Abass, Musaab Khudhur Mohammed, Fabrication of ZnO:Al/Si Solar Cell and Enhancement its Efficiency Via Al-Doping. *Nano Biomed. Eng.*, 2019, 11(2): 170-177.
DOI: 10.5101/nbe.v11i2.p170-177.

Abstract

In this work, zinc oxide (ZnO) and Al-doped ZnO (0.002, 0.004, and 0.006 wt.%) thin films were prepared by thermal evaporation technique with the thickness of about 125 nm. The X-ray diffraction (XRD) results showed that the prepared films were crystalline with a hexagonal wurtzite structure and preferential orientation in the (002) direction. The crystallite size increased with the increasing of Al doping. Atomic force microscopy (AFM) confirmed that the films grown by this technique had a good homogeneous surface. The roughness average, root mean square value, and the average grain diameter increased with the increasing of Al doping. The optical properties results showed that the transmittance increased with the increasing of Al doping, while the absorbance decreased. The pure and Al-doped ZnO thin films allowed direct energy gap (E_g) that was increased from 3.50 to 3.80 eV with the increasing of Al doping. The electrical properties of the films were studied, and it was found that all the prepared thin films were n-type and the mobility (μ) decreased with the increasing of Al doping. Current–voltage (I-V) characteristics showed that the highest efficiency was 3.64% with V_{oc} as of 2.8 V, I_{sc} as of 3.5 mA/cm^2 and F.F of 0.371 at the intensity of P =100 mW/cm^2..

Keywords: ZnO, Al, XRD, Optical properties, Thermal evaporation, Solar cell

Introduction

Solar power as a clean and economical energy source plays an important role in the 21st century in a low greenhouse gas future [1]. Zinc oxide (ZnO) is one of the II-VI compound semiconductors whose ionicity resides in being covalent and ionic semiconductor [2]. Due to its wide direct band gap (3.4 eV) [3], large excitation binding energy (60 meV) [4], excellent optical properties and low cost, ZnO has become one of the most important functional components in a plethora of devices [5].

The crystal structures of ZnO are wurtzite, rocksalt and zinc blende. Rocksalt and zinc blende are shown in Fig. 1 and 4, the thermodynamically stable phase is the wurtzite [6]. ZnO crystallize is favorably in the stable hexagonal wurtzite structure at room temperature and normal atmospheric condition [7]. It has lattice parameters a_o = 0.324 nm, c_o = 0.520 nm with a density of 5.60 g cm^{-3}. The electronegativity value of O^{-2} (3.44) and Zn^{+2} (1.65) causes very strong ionic bonding between Zn^{+2} and O^{-2} [8]. Its wurtzite structure is very simple to describe, where each oxygen ion is surrounded tetrahedrally by four zinc ions. It is clear that this kind of tetrahedral procedure of O^{-2} and Zn^{+2} in ZnO will form a non-central symmetric structure

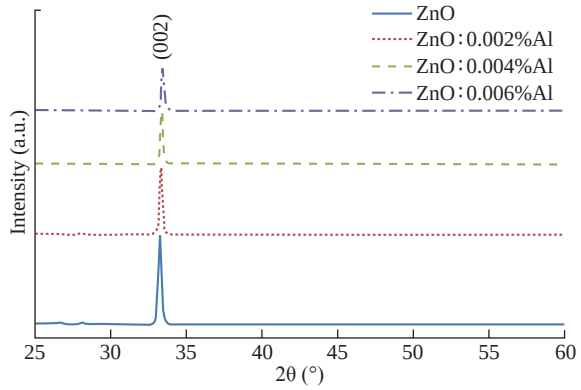

Fig. 1 The X-ray powder diffraction (XRD) pattern of pure and Al-doped ZnO thin films.

composed of two interpenetrating hexagonally closed packed sub-lattices of zinc and oxygen that are displaced with respect to each other by an amount of 0.375 along the hexagonal axis [9]. Various techniques such as pulsed laser deposition (PLD) [10], magnetron sputtering [11], chemical vapor deposition (CVD) [12], electron beam evaporation [13], hydrothermal method [14], and sol-gel process [15] have been applied to ZnO thin film preparation. The current research studied the effect of thickness and Al ratio on structural, morphological, optical, and electrical properties, fabricated solar cell from the prepared films, and measured its efficiency

Experimental

Fabrication of pure and ZnO Al-doped ZnO thin films with different Al-doping (0.002, 0.004, and 0.006) wt.% by thermal evaporation method on glass and silicon substrates. The thermal evaporation system is Edward C-306 deposition. The ZnO powder of 99.9% purity and the Al powder of 99.9% purity were used as source materials molybdenum boat. The chamber was evacuated down to 1×10^{-7} mbar. The source to substrate distance was about 15 cm. The films were annealed at temperatures of 573 K for 2 h. The structure of the films was characterized by a SHIMADZU X-ray diffractometer system (XRD-6000) with a source CuK_{α} with radiation of wavelength $\lambda = 1.5406$ Å. The surface roughness was analyzed by a Aα3000 scanning probe microscopy (AFM), spectrophotometer (Shimadzu UV-1650 PC) made by Phillips (Japan) to record transmission scales of the ZnO:Al thin films in the wavelength range of 200 to 1100 nm, based on Van der Pau method. The electrical properties were determined by an HMS 3000 Hall measurement system. The thickness of the films was measured to be 125 nm by optical thin film measurement with Lambda Limf-10.

Results and Discussion

The X-ray powder diffraction (XRD) pattern for pure and Al-doped ZnO thin films are shown in Fig. 1. A peak was obtained at $2\theta = 33.25°$, which corresponds to the (002) for pure ZnO taken from the Joint Committee of Powder Diffraction Standard (JCPDS) card file data (79-2205) [16]. This indicates that ZnO, both pure and doped with Al films prepared by thermal evaporation technique, showed a good c-axis orientation perpendicular to the substrate with a hexagonal wurtzite type crystal structure and the behavior of increased degree of crystallinty of films. The results are in good agreement with researches conducted by Mugwanga et al. and Kumar et al. [17, 18]. The intensity of peak (002) decreased with the increasing of Al doping, which is in good agreement with the finding by Pogrebnjak et al. [19]. And the diffraction peak of (002) planes of doped films shifted to higher angle, which suggests Al doping at the Zn sites in the ZnO crystal because of the ionic radius of Al^{3+} (0.054 nm) [20] was smaller as compared with that of Zn^{2+} (0.074 nm) [20], which is in good agreement with the finding by Oku et al. [20]. A full-width at half maximum (FWHM) of the (002) peaks decreased slightly with the increasing of Al doping. This finding indicates that the samples had a certain crystalline quality. The measured FWHM of the samples was 0.245° to 0.109°. The crystallite size of the pure ZnO and Al-doped ZnO thin film was calculated from the (002) diffraction peak using Scherer's formula according to the following equation [21]:

$$D = 0.9\lambda / \beta \cos\theta.$$

The crystallite size for pure and Al-doped ZnO thin films deposited on glass substrate was calculated to be 33.858 to 76.133 nm. Our results are in good agreement with that reported by Wan et al. [22]. The results are listed in Table 1.

Table 1 The obtained results of the X-ray powder diffraction (XRD) for pure and Al-doped ZnO thin films

ZnO:Al (wt.%)	2θ (°)	hkl	FWHM (degree)	Crystallite size (nm)
0	33.25	002	0.245	33.858
0.002	33.30	002	0.174	47.679
0.004	33.35	002	0.201	41.280
0.006	33.40	002	0.109	76.133

The atomic force microscopy (AFM) images of pure and Al-doped ZnO thin films show a uniform granular surface morphology. From Figs. 2-5, it can be observed that the roughness increased from 2.73 nm for pure ZnO to 3.11 nm for ZnO:0.006% Al thin film. This result could be probably due to the increasing concentration of aluminum atomic in the ZnO thin films. The root mean square (RMS) increased with the increasing of Al doping, which is in accordance with the findings by Vinodkumar et al. and Tseng et al. [23, 24]. The average grain diameter was evaluated from the plane view images that increased from 56.1 nm for pure ZnO to 109.4 nm for ZnO:0.006% Al thin films. The tilted image exposes grain heights of a few tens of nanometers, as shown in Table 2.

Ultraviolet-visible spectrophotometer in the wavelength range of 200-1100 nm was used to determine the optical properties, such as transmittance, absorption coefficient (α), and optical energy gap (E_g). From Fig. 6, it can be observed that the transmittance increased with the increasing of Al doping in the

Table 2 Morphological characteristics of ZnO:Al thin films at different Al-doping and annealing temperature at 573 K

Al-doped (wt.%)	Roughness average (Sa) (nm)	Root mean square (Sq) (nm)	Ten point height (Sz) (nm)	Average diameter (nm)
0	2.73	3.42	8.92	56.1
0.002	2.91	3.77	9.65	69.2
0.004	2.61	3.33	9.18	98.6
0.006	3.11	4.06	11.20	109.4

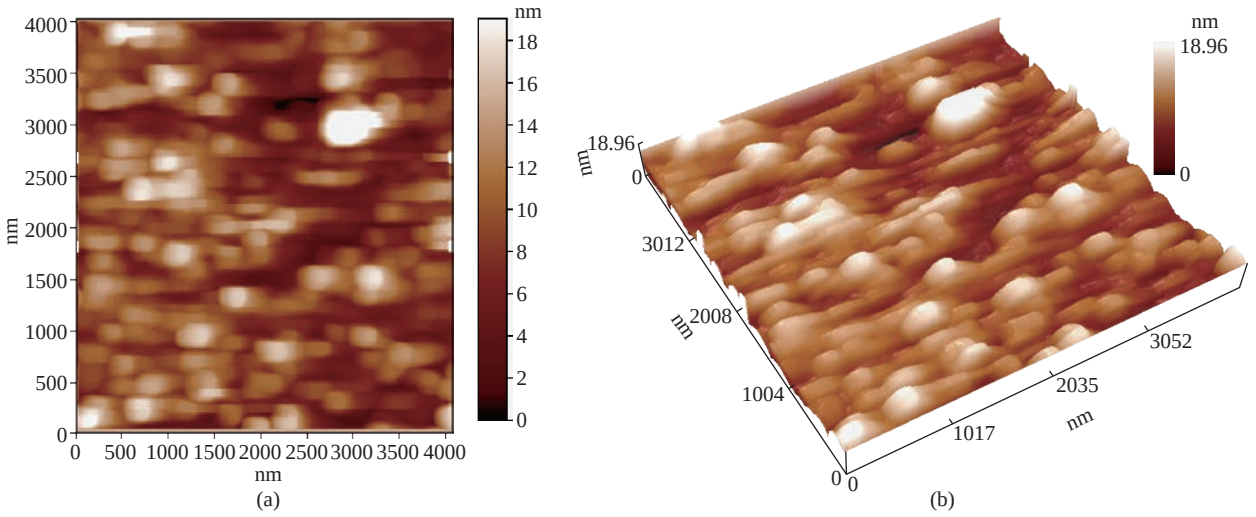

Fig. 2 AFM images of pure ZnO thin film with annealing temperature at 573 K for **(a)** 2-D and **(b)** 3-D.

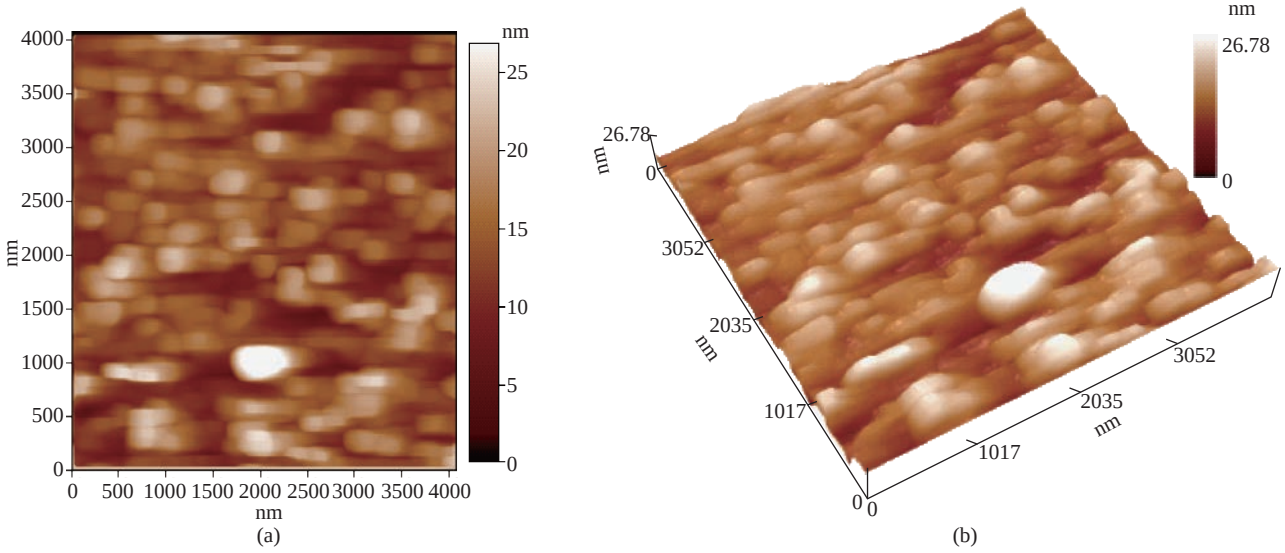

Fig. 3 AFM images of ZnO:0.002% Al thin film with annealing temperature at 573 K for **(a)** 2-D and **(b)** 3-D.

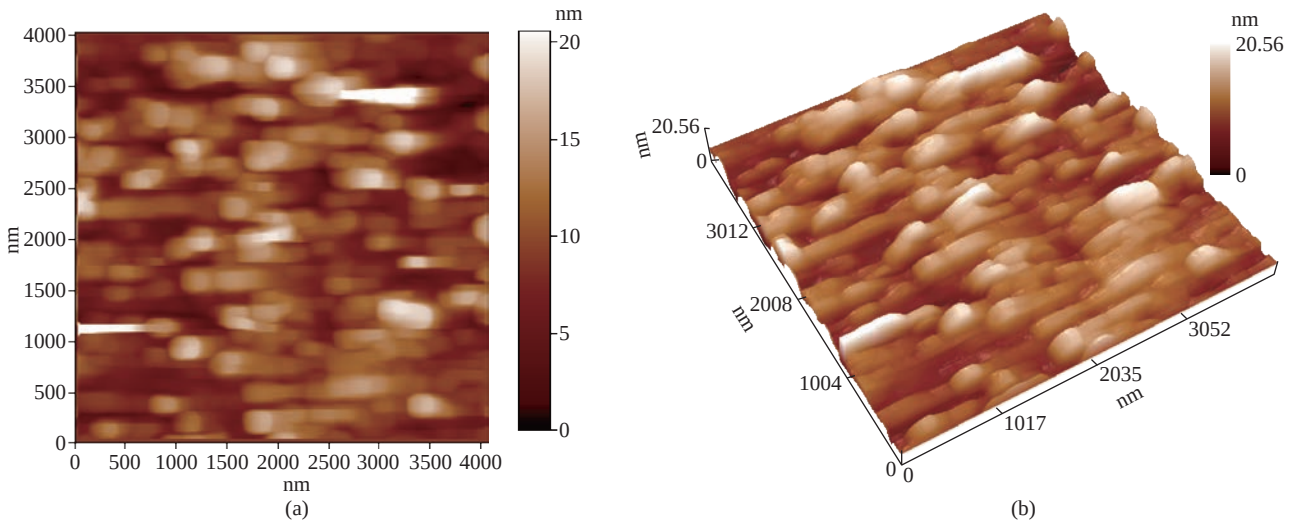

Fig. 4 AFM images of ZnO:0.004% Al thin film with annealing temperature at 573 K for **(a)** 2-D and **(b)** 3-D.

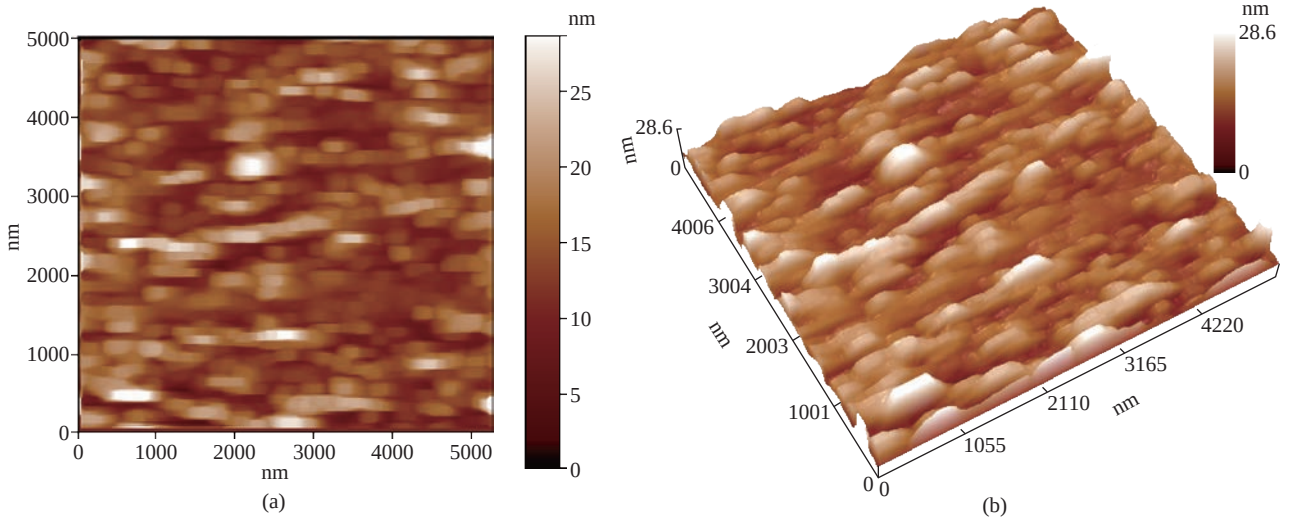

Fig. 5 AFM images of ZnO:0.006% Al thin film with annealing temperature at 573 K for **(a)** 2-D and **(b)** 3-D.

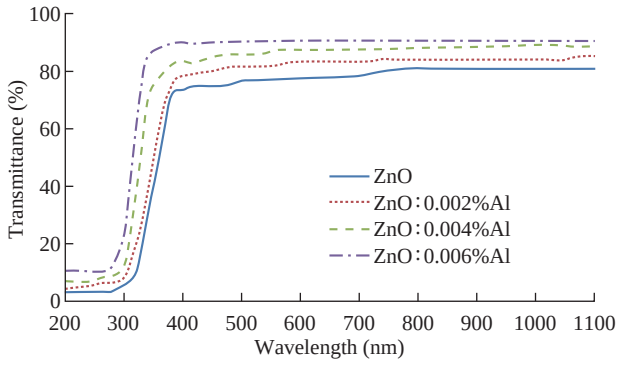

Fig. 6 Transmittance spectra as a function of the wavelength of ZnO:Al thin films.

ZnO:Al thin films. This result may be due to the reduction of voids in the sample and the improvement of homogeneous structure with uniformly distributed particles, thereby increasing the optical scattering. The increased optical transmittance was related to the crystallinity of the films, which is in accordance with the findings by Chopra et al. and Mkawi et al. [25, 26].

Fig. 7 illustrated the absorbance spectra of pure and Al-doped ZnO thin films with different Al doping. It can be observed that the absorbance decreased with the increasing of Al-doping for the prepared thin films.

The absorption coefficients of pure and Al doping ZnO films were calculated by using the equation [27]:

$\alpha = 2.303\ A/t.$

From Fig. 8, it can be observed that the absorption coefficient decreased with the increasing of Al doping. The values were larger than 10^4/cm, which caused increase of probability of the occurrence of direct transitions. This can be linked with the increase in grain size and it may be attributed to the light scattering effect for its high surface roughness, which

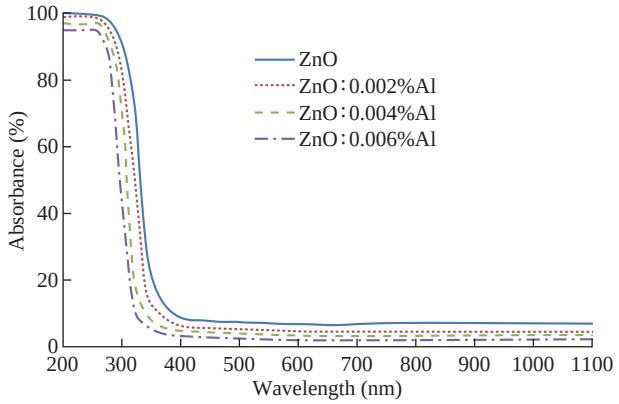

Fig. 7 The absorbance spectra as a function of wavelength of ZnO:Al thin films.

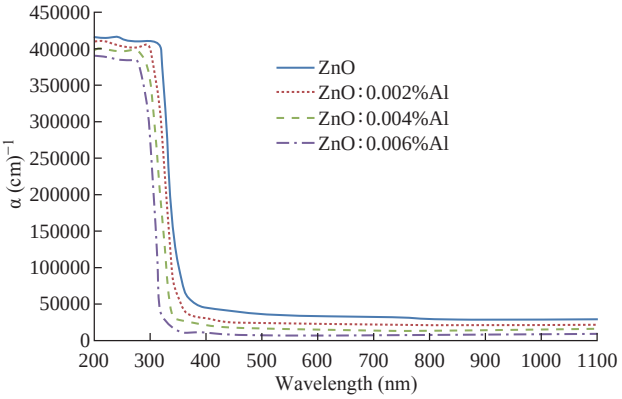

Fig. 8 The absorption coefficient spectra as a function of wavelength of ZnO:Al thin films.

is in agreement with the finding by Alnajjar [25] and Karvinen [28].

The optical energy gap of ZnO:Al thin films was determined by using the equation [26]:

$(\alpha h\nu)^2 \approx [\, h\nu - E_g \,]$.

The plot of $(\alpha h\nu)^2$ with energy ($h\nu$) indicates that ZnO films are direct transition type semiconductors for the thin films. The photon energy at the point where $(\alpha h\nu)^2$ is E_g. Fig. 9 shows the energy gap of pure and Al-doped ZnO films with various Al doping (0.002, 0.004, and 0.006) wt.%. An obvious increase was observed in the values of the energy

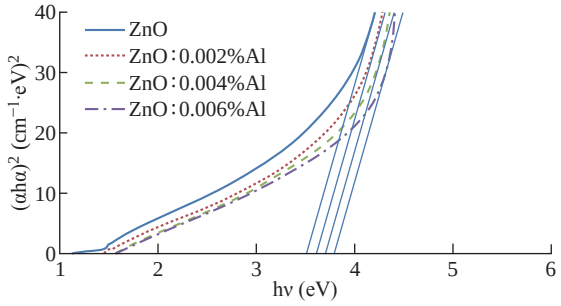

Fig. 9 A plots of $(\alpha h\nu)^2$ verses photon energy ($h\nu$) of ZnO:Al thin films at different Al-doping ratio.

Table 3 The results of optical energy gap of pure and Al-doped ZnO films

Type of the film	Optical energy gap (eV)
ZnO pure	3.50
ZnO:Al 0.002%	3.62
ZnO:Al 0.004%	3.72
ZnO:Al 0.006%	3.80

gap with the increasing of Al doping. The increase is explained by the preposition that the ZnO:Al films are semiconductors in which the Fermi level lies in the conduction band, which means the levels at the bottom of the conduction band were occupied by electrons. The shielding electrons traveling to these levels leading to transferring the electrons from valence to conduction band is termed the Burstein-Moss effect. These results showed a good agreement with the findings by Youssef et al. [27] and Moss [28]. The values of E_g are listed in Table 3.

Hall voltage parameters were examined for ZnO and Al-doped ZnO thin films prepared by thermal evaporation technique by using Van der Pau method. The Hall parameters, such as Hall coefficient (R_H), carrier concentrations (n), electrical conductivity (σ), and Hall mobility (μ_H) were determined by using Van der Pau system, as tabulated in Table 4. It is obvious that the Hall coefficient decreased with the increasing of Al doping. However, carrier concentration of the samples increased with the increasing of Al doping. This behavior has been explained according to the

Table 4 Result of Hall measurement for pure and Al-doped ZnO films

Al-doped ZnO (wt.%)	R_H (cm^3/C)	Carrier type	n $(cm)^{-3}$	σ (1/Ω.cm)	μ_H (cm^2/V.s)
0.000	-8.247×10^{7}	n	7.569×10^{10}	1.210×10^{-5}	12.88×10^{3}
0.002	-2.114×10^{7}	n	2.953×10^{11}	1.636×10^{-5}	6.317×10^{3}
0.004	-3.125×10^{6}	n	1.997×10^{12}	1.561×10^{-4}	4.81×10^{3}
0.006	-2.877×10^{6}	n	2.170×10^{12}	1.153×10^{-3}	3.317×10^{3}

normal doping rules, i.e. substitution of Al^{3+} at the Zn^{2+} sites creates one extra free carrier in the process and all samples exhibit n-type, which is in accordance with the findings by Rahman et al. [29].

The electrical conductivity of ZnO and Al-doped ZnO thin films increased with the increasing of Al doping, which was explained by the increase in carrier concentration. From Fig. 10, it is found that the Hall mobility of ZnO and Al-doped ZnO thin films decreased with the increasing of Al doping, and the decrease in the mobility of carriers may have been due to the ionized impurity scattering and the decreased mobility of carriers caused by high carrier concentration, which is in accordance with the findings by Wan et al. [22] and Wang et al. [30].

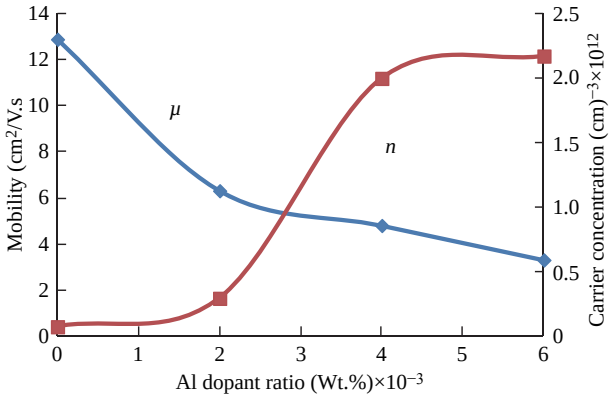

Fig. 10 The variation of mobility and carrier concentration of ZnO and ZnO:Al thin films.

The junction of ZnO:Al/p-Si was formed by the thermal evaporation technique, and studied with I-V curves which were of various behaviors according to the ambient of preparing the junction as presented in Fig. 11.

Anisotype n-p heterojunction (HJ) would be obtained by ZnO:Al/p-Si for 0.002, 0.004 and 0.006 wt.%, because ZnO:Al are n-type and Si is p-type.

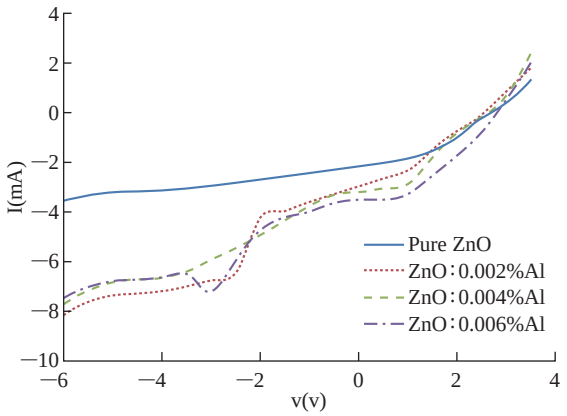

Fig. 11 I-V characteristic for pure and Al-doped ZnO films and doped with P = 100 mW/cm^2.

The I-V curves of ZnO:Al/p-Si heterojunction are illustrated in the figures. The I-V of ZnO:Al/p-Si HJ was characterized at forward bias voltage for different Al doping within the range of -8 to4 V. These curves exhibited the behavior of the current with the forward and reverse bias voltage. The current-voltage characteristics under illumination was one of the optoelectronic typical for HJ. The measurements were taken under incident power densities equal to 100 mW/cm^2.

From Fig. 11, it is obvious that the photocurrent increased with the increasing of bias voltage. It also can be seen that the photocurrent in the reverse bias was larger than that in the forward bias. This could be attributed to the fact that the width of the depletion region increased with the increasing of the applied reverse bias voltage that led to the separation of the electron–hole pairs. The efficiency increased with the increasing of Al-doping and could be obtained with an increase in Al doping. The highest efficiency at doping 0.006 wt.% was 3.64 % with V_{oc} of 2.8 V, I_{sc} of 3.5 mA/cm^2 and F.F of 0.371. The improved device performance was caused by the high I_{sc} and V_{oc} of this device. The results are listed in Table 5. The Al-doping increased the energy conversion efficiency by retarding

Table 5 Results of the I-V for Al doped ZnO thin films with various doping at temperature 573 K.

Al-doped ZnO (wt.%)	I_{sc} (mA/cm^2)	V_{oc} (v)	I_{max} (mA)	V_{max} (v)	F.F	η(%)
0	2.167	2.65	1.65	1.30	0.390	2.14
0.002	2.983	2.55	2.00	1.20	0.315	2.40
0.004	3.200	2.68	2.05	1.40	0.334	2.87
0.006	3.500	2.800	2.80	1.30	0.371	3.64

the electron-hole recombination. These results reveal that the extrinsic influences, such as specific surface area, are very important to improve the performance of ZnO:Al solar cells.

Conclusions

The films of pure and Al-doped ZnO were successfully prepared by thermal evaporation technique on glass and silicon substrates. From XRD, the crystalline was satisfied with a hexagonal wurtzite structure and preferential orientation in the (002) direction. The crystallite size increased with the increasing of Al doping. From AFM measurement, a uniform granular surface showed morphology of the atomic force microscope (AFM) images of thin films. The roughness average and root mean square increased with the increasing of Al doping. The optical properties results showed that the transmittance increased with the increasing of Al doping, while the absorption coefficient decreased. The optical measurement showed that the pure and Al-doped ZnO thin films allowed direct energy gap (E_g) that increased from 3.50 to 3.80 eV with the increasing of Al doping. Hall measurements indicated that the films were n-type semiconductors and found that the carrier concentration (n) and electrical conductivity (σ) increased with the increasing of Al doping, while the mobility (μ) decreased. The high conversion efficiency (η) was 3.640% for 0.006% Al-doped ZnO thin film.

References

[1] U. Ozgür, Y.I. Alivov, C. Liu, et al., A comprehensive review of ZnO materials and devices. *J. of Applied Phys.*, 2005, 98: pages.

[2] J.A. van de Walle, Fundamentals of zinc oxide as a semiconductor. *Rep. Prog. Phys*., 2009, 72: 126501-126529.

[3] K. Mishjil, S. Chiad, H. Khalid, et al., Effect of Al doping on structural and optical parameters of ZnO thin films. *Materials Focus*, 2016: 471-475.

[4] J. Wang, V. Sallet, F. Jomard, et al., Influence of the reactive N_2 gas flow on the properties of rf-sputtered ZnO thin films. *Thin Solid Films*, 2007, 515(24): 8780-8784.

[5] M.H. Huang, S. Mao, H. Feick, et al., Room-temperature ultraviolet nanowire nanolasers. *Science*, 2001, 292(5523): 1897-1899.

[6] H. Morkoc, U. Ozgur, General properties of ZnO, zinc oxide: fundamentals. *Materials and Device Technology*, 2009: 1-2.

[7] V.A. Colemen, C. Jagadish, Zinc oxide bulk, thin films and nanostructures. *Materials Sci. Eng.*, 2006, 978(8): 1-22.

[8] A.L. Allenic, Structural, electrical and optical properties of p-type ZnO Epitaxial films. Ph.D thesis, University of Michigan, 2008.

[9] H.B. Abdul Hamid, Fabrication, structural and electrical characteristics of zinc oxide (ZnO). Ph.D. thesis, University Sains Malaysia, 2009.

[10] M. Grundmann, H. von Wenckstern, R. Pickenhain, et al., Electrical properties of ZnO thin films and single crystals. *Zinc Oxide - A Material for Micro- and Optoelectronic Applications*, 2003: 47-57.

[11] P.F. Carcia, R.S. McLean, M.H. Reilly, et al., Transparent ZnO thin-film transistor fabricated by rf magnetron sputtering. Applied Physics Letters, 2003, 82: 1117.

[12] C.R. Gorla, N.W. Emanetoglu, S. Liang, et al., Ultraviolet detectors based on epitaxial ZnO films grown by MOCVD. *J. Appl. Phys.*, 2000, 29(1): 69-74.

[13] M.S. Kim, K.G. Yim, S.M. Jeon, et al., Effects of annealing atmosphere and temperature on properties of ZnO thin films on porous silicon grown by plasma-assisted molecular beam epitaxy. *J. Appl. Phys.*, 2012, 8(2): 123-129.

[14] M.S. Kim, K.G. Yim, J.Y. Leem, et al., Hydrothermally grown boron-doped ZnO nanorods for various applications: Structural, optical, and electrical properties. *J. Korean Phys. Soc., Electronic Materials Letters*, 2014, 10(1): 81-87.

[15] M. Singh, M. Singh, Equation of state for the study of temperature dependence of volume thermal expansion of nanomaterials. *Science and Education*, 2001, 80: 383.

[16] Joint Committee for Powder Diffraction Standards, Power Diffraction File for Inorganic Materials, 1979, 79-2205.

[17] F.K. Mugwanga, P.K. Karimi, W.K. Njoroge, et al., Characterization of aluminum doped zinc oxide (AZO) thin films prepared by reactive thermal evaporation for solar cell applications. *J. of Fundamentals of Renewable Energy and Applications*, 2015, 5: 2-6.

[18] G.A. Kumar, M.V. Ramana, and K.N. Reddy, Structural and optical properties of ZnO thin films grown on various substrates by rf magnetron sputtering. Proceedings of the International Conference on Materials Science and Technology, 2015, 73.

[19] A.D. Pogrebnjak, A.A. Muhammed, E.T. Karash, et al., Effects of Al dopant on structural and optical properties of ZnO thin films prepared by sol-gel. *Przeglad Elektrotechiczny*, 2013, 89: 315-317.

[20] T. Oku, Y. Tetsuya, F. Kazuya, et al., Microstructures and photovoltaic properties of ZnO:Al/Cu_2O-based solar cells prepared by spin-coating and electrodeposition. *Solar Energy Materials & Solar Cells*, 2014, 4: 203-213.

[21] C. Gumus, O.M. Ozkendir, H. Kavak, et al., Structural and optical properties of zinc oxide thin films prepared by spray pyrolysis method. *J. Optoelectronics and Advanced Materials*, 2006, 8: 299-303.

[22] D. Wan, F. Huang, and Y. Wang, Highly surface-textured ZnO:Al films fabricated by controlling the nucleation and growth separately for solar cell applications. *Am. Chem. Soc.*, 2010, 2: 2147-2152.

[23] R. Vinodkumar, I. Navas, S.R. Chalana, et al., Highly conductive and transparent laser ablated nanostructured Al:ZnO thin films. *Appl. Surface Sci.*, 2010, 257(3): 708-716.

[24] C.A. Tseng, J.C. Lin, Y.F. Chang, et al., Microstructure and characterization of Al-doped ZnO films prepared by rf power sputtering on Al and ZnO targets. *Appl. Surface Sci.*, 2012, 258(16): 5996-6002.

[25] K.L. Chopra, *Thin films phenomena*. Mc. Graw-Hill, NewYork, 1969.

[26] E.M. Mkawi, K. Ibrahim, M.K. Ali, et al., The effect of dopant concentration on properties of transparent conducting Al-doped ZnO thin films for efficient Cu_2ZnSnS_4 thin film solar cells prepared by electrodeposition method. *Appl. Nanosci*, 2015, 5: 993-

1001.
[27] J.I. Pankove, *Optical process in semiconductors*. Dover Publishing, Inc., New York, 1971.
[28] S. Karvinen, The effect of trace element doping of TiO_2 on the crystal growth and on the anatase to rutile phase transformation of TiO_2. *Solid State Sci.*, 2003, 5: 811-819.
[29] A.A. Alnajjar, ZnO:Al grown by sputtering from two different target sources. A comparison study. *Advances in Condensed Matter Phys*, 2012, 2012.
[30] J. Marien, T. Wagner, G. Duscher, et al., Ag, Pt, Pd, Nb doping (110) TiO_2 (Rutile), growth, structure, and chemical composition of the interface. *Surface Sci.*, 2000, 446: 219.
[31] A. Youssef, L. Abdelrrazak, H. Bouchaib, et al., Structural, optical and electrical properties of ZnO:Al thin films for optoelectronic applications. *Optical and Quantum Electron*, 2014, 46: 229-234.
[32] T.S. Moss, The interpretation of the properties of indium antimonide. *Proc. Phys. Soc. Lond. Sect. B*, 1954, 67: 775-782.
[33] M.M. Rahman, M.K. Khan, M.R. Islam, et al., Effect of Al doping on structural, electrical, optical and photoluminescence properties of nano-structural ZnO thin films. *J. Materials Sci. Technol.*, 2012, 28(4): 329-335.
[34] A. Wang, T. Chen, S. Lu, et al., Effects of doping and annealing on properties of ZnO films grown by atomic layer deposition. *J. of Nanoscale Research Letters*, 2015, 10: 75.